c_y

VARIATION OF H_2O AND CO_2 CRYODEPOSIT REFLECTANCES WITH ANGLE OF INCIDENCE AND DEPOSIT THICKNESS

B. E. Wood, A. M. Smith, and B. A. Seiber

ARO, Inc.

September 1968

AEROSPACE ENVIRONMENTAL FACILITY
ARNOLD ENGINEERING DEVELOPMENT CENTER
AIR FORCE SYSTEMS COMMAND
ARNOLD AIR FORCE STATION, TENNESSEE

NOTICES

VARIATION OF H₂O AND CO₂ CRYODEPOSIT REFLECTANCES WITH ANGLE OF INCIDENCE AND DEPOSIT THICKNESS

B. E. Wood, A. M. Smith, and B. A. Seiber

ARO, Inc.

This document has been approved for public release and sale; its distribution is unlimited.

FOREWORD

The research reported herein was sponsored by Headquarters, Arnold Engineering Development Center (AEDC), Air Force Systems Command (AFSC), Arnold Air Force Station, Tennessee, under Program Element 6144501F, Project 8951, Task 895104.

The results of the research presented were obtained by ARO, Inc. (a subsidiary of Sverdrup & Parcel and Associates, Inc.), contract operator of the AEDC, AFSC, under Contract F40600-69-C-0001. The research was conducted from May 1966 to April 1968 under ARO Project No. SW5803, and the manuscript was submitted for publication on June 10, 1968.

This technical report has been reviewed and is approved.

Terry L. Hershey
Captain, USAF
Research Division
Directorate of Plans
  and Technology

Edward R. Feicht
Colonel, USAF
Director of Plans
  and Technology

ABSTRACT

Cryodeposits which form on the cryogenically cooled walls of a space simulation chamber can change the wall reflectance and thus alter the thermal balance of the test vehicle. In this study, H_2O and CO_2 cryodeposits of thicknesses up to 1.8 mm were formed on a 77°K surface under vacuum. The spectral reflectances of these deposits were measured in situ with an integrating sphere for angles of incidence from 0 to 60 deg. At the smaller deposit thicknesses, the reflectance showed a strong dependence on both thickness and angle of incidence, whereas at larger thicknesses the dependence was less. A theoretical model developed for reflectance determination of absorbing and scattering media gives a good representation of the thickness dependence of water cryodeposit reflectance except at very small thicknesses where interference effects are known to occur.

CONTENTS

APPENDIX
Illustrations

NOMENCLATURE

A_c	Total cryopumping area
$B_{\lambda, MgO}$	Detector output obtained from radiation incident on MgO reference surface
$B_{\lambda, s}$	Detector output obtained from radiation incident on the sample
D	Density of cryodeposit
LN_2	Liquid nitrogen
ℓ	Thickness of absorbing and scattering media in Ref. 8
ℓ_{av}	Thickness of cryodeposit
$\dot{m}$	Mass flow rate
R	Calculated reflectance, from Ref. 8
r	Reflectance of substrate in Ref. 8
t	Time
β	Absorption coefficient
η	Fraction of radiation scattered forward
λ	Wavelength
$\rho_{\lambda, MgO}$	Measured spectral reflectance of MgO reference surface
$\rho_{\lambda, s}$	Measured spectral reflectance of the sample
σ	Scattering coefficient
ψ	Angle of incidence measured from the surface normal

SUBSCRIPTS

c	Denotes collimated radiation
d	Denotes diffuse radiation

SECTION I
INTRODUCTION

Space simulation in ground test facilities requires the chamber walls to be black to maximize the absorption of the incident solar simulator radiation. To reduce chamber wall emission and increase the system pumping capacity, the walls are cooled to a temperature near 77°K. However, the cryopumping of gases by these cold surfaces forms cryodeposits which will alter the wall reflective properties. This change in wall reflectance may influence the degree of space simulation, but the thermal test data can be corrected by knowing the radiative properties of the cryodeposits. These properties will depend on the cryodeposit thickness, the incidence angle and wavelength of the incident radiation, the substrate material, and the temperature and pressure at which the deposits were formed. The dependence of cryodeposit reflectance on wavelength has been previously discussed in Refs. 1 - 4. This work is concerned primarily with the effects of the other parameters and of test gas flow rate and cryodeposit species. For normal space chamber operation, the cryodeposits most likely to form on 77°K surfaces are water and carbon dioxide. Therefore, these were the two cryodeposit species investigated.

SECTION II
EXPERIMENTAL APPARATUS AND PROCEDURE

To measure the reflectance of a surface, the radiation incident on the surface and the radiation reflected must be known. For specular reflecting surfaces, capturing all of the reflected energy is a relatively simple matter, but for diffuse reflecting surfaces some kind of hemispherical collector is required. For this reason, integrating spheres and hemispherical reflectometers have been found to be the most convenient and accurate systems for obtaining reflectances of diffuse and semidiffuse (not perfectly specular) surfaces. Since cryodeposits are essentially diffuse reflectors for wavelengths in the solar region, one of the two aforementioned systems was required for cryodeposit reflectance measurements. The integrating sphere was chosen since its theory is well established and vacuum connections could be conveniently made to a sphere. Normally, an integrating sphere is operated at atmospheric conditions. However, since space chamber cryodeposits are formed in vacuum, the deposits investigated in this study had to be similarly formed. The reflectance measurements also had to be made in situ since subsequent exposure to atmosphere could alter the deposit by formation of impurities and change of the crystal structure.

A 12-in.-diam integrating sphere was fabricated and coated internally with magnesium oxide (MgO) approximately 1 to 2 mm thick. The sphere was composed of two flanged hemispheres which were vacuum sealed by an O-ring (Fig. 1). It was mounted on a vacuum system equipped with a 4-in.-diam oil diffusion pump and an ion pump. Either or both of the pumps could be valved off from the sphere. With this vacuum system, pressures in the low 10^{-7} torr range could be easily achieved. The test surface was one face of a hollow copper cryopump, 1 by 1-1/2 by 2-1/2-in. in outside dimensions, which could be cooled to approximately 77°K by circulating liquid nitrogen (LN$_2$) through it. To limit cryopumping to the copper cryosurface, the LN$_2$ transfer lines were vacuum jacketed. The 1-1/2- by 2-1/2-in. face used as a test surface was either maintained as a bare polished copper surface or coated with a selected black epoxy paint. All other portions of the cryopump surface and the vacuum-jacketed transfer lines were smoked with MgO. The cryopump could be rotated through 270 deg so that either the front or back surface could be illuminated. This allowed the opposite side of the test surface to be used as the MgO reference surface and reflectance measurements to be made for various angles of incidence.

The test surface was irradiated with monochromatic radiation by the optical arrangement shown in Fig. 2. Radiation from a 200-w tungsten-iodine lamp was focused on the entrance slit of a single-pass Perkin-Elmer monochromator having a calcium fluoride prism as the dispersing element. The monochromatic radiation was then focused on the test surface by an off-axis mirror. By using a magnification of 1, the irradiated test surface area was identical to the monochromator slit area, 0.5 by 12 mm. Intensity measurements of the radiation on the sphere wall were obtained using an end-on photomultiplier tube which has an S-1 response and is sensitive to wavelengths between 0.35 and 1.2 μ.

The reflectance measurements were made using the angular-hemispherical technique. In this technique (Fig. 3) monochromatic radiation is incident on the test surface at a given angle ψ, measured from the surface normal, and the radiation reflected strikes the hemisphere facing the test surface and is then reflected diffusely throughout the sphere. After multiple reflections within the sphere, the intensity at the wall is measured by the photomultiplier tube to obtain an output value $B_{\lambda, s}$. The test surface is then rotated 180 deg so that the radiation entering the sphere is incident on the MgO coating on the back side of the test surface. The energy reflected from the MgO surface is similarly detected, and the reading $B_{\lambda, MgO}$ is taken as the reference value for that particular wavelength. It should be noted that the detector

does not view the first reflection from the wall for either the sample or reference measurements. From the two detector readings, $B_{\lambda,s}$ and $B_{\lambda,MgO}$, the spectral reflectance $\rho_{\lambda,s}$ of the test surface can be determined from the equation

$$\frac{\rho_{\lambda,s}}{\rho_{\lambda,MgO}} = \frac{B_{\lambda,s}}{B_{\lambda,MgO}} \tag{1}$$

From Eq. (1) it is seen that the ratio of $B_{\lambda,s}$ to $B_{\lambda,MgO}$ gives the spectral reflectance relative to the MgO reflectance at the same wavelength. However, the reflectance of MgO is near unity (from 0.95 to 0.98) over the wavelength range investigated, and, hence, the relative reflectance values can be interpreted as approximate absolute values.

Before each set of experiments, the interior of the integrating sphere and all areas in the cryopump assembly except the test surface were cleaned and recoated with MgO. In this manner freshly prepared MgO coatings were always used. The pressure in the chamber was then reduced from atmosphere to approximately 10^{-5} torr using the diffusion pump, after which it was valved off and the ion pump started. The ion pump has the advantage that the further possibility of oil backstreaming is eliminated. The base pressure obtained in the system was about 1×10^{-7} torr. After the pressure in the system stabilized, reflectance measurements were made as functions of wavelength and angle of incidence for the test surface at room temperature (300°K). Similar measurements were made for the MgO surface at 300°K and were taken as the reference values for all cryodeposit reflectance measurements made during the experiment. After completion of these measurements, the LN_2 flow was started and the test surface cooled to 77°K. Then reflectance measurements were made again. At this point the ion pump was shut off and a known flow rate of test gas, either H_2O or CO_2, was started. As the gas entered the sphere, it was cryopumped by the LN_2-cooled cryosurface, forming a deposit over the entire surface area. At the end of a specified time interval, the flow of test gas was stopped. After time was allowed for the remaining gas in the chamber to be cryopumped, reflectance measurements were made for the test surface which was now coated with a layer of cryodeposit. On completion of the measurements, the flow of the test gas was again started and a thicker layer formed. This procedure was continued until the cryodeposit reflectance had essentially reached a plateau. At this plateau, the cryodeposit thickness was from 1 to 2 mm, depending on the cryodeposit species and the angle of incidence and wavelength of the radiation.

The cryodeposit thickness was calculated from the following equation:

$$\ell_{av} = \frac{\dot{m}t}{A_c D}$$ (2)

where ℓ_{av} is the average thickness over the entire cryosurface, $\dot{m}$ is the mass flow rate of the test gas, t is the time of flow, A_c is the entire surface area of the cryosurface, and D is the cryodeposit density. A density of 1.5 gm/cm^3 was taken for the CO_2 deposits since they were formed at pressures between 10^{-3} and 1 torr (Ref. 2), and the density of the water deposits was assumed to be 0.9 gm/cm^3 (Ref. 5). The H_2O deposits were formed for water vapor flow rates of 1.01 x 10^{-3} gm/sec and 1.44 x 10^{-3} gm/sec. The CO_2 deposits were formed at flow rates of 2.4 x 10^{-3} gm/sec and 2.6 x 10^{-4} gm/sec.

During deposition the chamber pressures varied from 10^{-3} to 1 torr and depended on the flow rate, species of the test gas, and thickness of the cryodeposit which had already been formed. In general, the rate of pressure rise increased with deposit thickness, indicating that the capture coefficient decreased as the thickness increased. This increased rate of pressure rise was not due to a buildup of condensable gas impurities since these were removed by the diffusion pump before each set of reflectance measurements.

SECTION III
RESULTS AND DISCUSSION

3.1 THIN FILM EFFECTS (0 to 0.05-mm Thick)

Variations in test vehicle temperatures due to cryodeposits on space chamber walls will generally be insignificant for deposit thicknesses less than from 75 to 100μ. Therefore, most of this study was concerned with deposits greater than 100μ thick. There were, however, some investigations made for thin films of H_2O and CO_2 cryodeposits. Interference reflectance patterns were noted for both H_2O and CO_2 films formed on the black paint and polished copper surfaces. Figure 2 shows an example of the thin film interference patterns observed for a water cryodeposit film formed on a black epoxy substrate. The reflectance is shown as a function of the time of flow of the test gas which, in turn, can be related to the film thickness. The 77°K black surface had an initial reflectance of 5 percent and, as seen in Fig. 4, this was reduced to 1.5 percent at the first interference minimum. The film thickness at which this occurs is $\lambda/4n$ where λ is the

wavelength of the incident radiation, $0.52\,\mu$, and n is the film refractive index, 1.31. Therefore, the first minimum for this particular case occurred at a film thickness of approximately $0.1\,\mu$. After the interference patterns died out, the reflectance continued to decrease until a minimum of approximately 3.2 percent was reached at a deposit thickness of about $15\,\mu$. For deposit thicknesses greater than this, the reflectance increased, and at a thickness of about 30 to $40\,\mu$, the original reflectance value of the bare surface, 5 percent, was reached. The reflectance then continued to rise with increasing deposit thickness.

In addition to the thin film interference patterns, scattering interference patterns have been observed in angular distribution measurements of reflected radiation from thin cryodeposits (Ref. 2). These scattering patterns have been observed for thicknesses of up to $100\,\mu$, whereas the thin film reflectance patterns for visible radiation die out at much smaller thicknesses. These two types of interference phenomena have proved to be valuable in the determination of cryodeposit refractive index, thickness, and density (Ref. 2).

3.2 WATER CRYODEPOSITS (0.11 to 1.32 mm Thick)

In contrast to the results obtained for thin cryodeposit films, significant changes in reflectance were observed for water cryodeposits between 0.11 and 1.32 mm thick. The reflectances of water cryodeposits formed on an LN_2-cooled black epoxy paint surface are shown as a function of deposit thickness and wavelength in Figs. 5a through d for radiation incidence angles of ψ = 0, 20, 40, and 60 deg, respectively. For this series of tests the flow rate of the water vapor was 1.01×10^{-3} gm/sec. It is apparent that for small deposit thicknesses, the reflectance increase is much greater at the shorter wavelengths, as seen in Fig. 5a. For example, at a deposit thickness of 0.22 mm, the $0.4\text{-}\mu$ reflectance curve has increased from an initial value of 4 percent up to 79 percent, whereas the $1.15\text{-}\mu$ wavelength curve shows an increase up to only 23 percent. For deposit thicknesses between 0.22 and 0.66 mm, the reflectance continues to increase, and at 0.88 mm it appears that the reflectance has reached a plateau where any further thickness increase will not affect its value. However, increasing the thickness to 1.32 mm caused a sharp rise in the cryodeposit reflectance to the point where it was essentially equivalent to that of MgO. This increase was probably caused by a change in the formation properties of the deposit, such as crystal structure or particle size.

From Figs. 5a through d the shape of the reflectance curves is seen to be independent of the incidence angle, although in most cases the overall reflectance level was higher for the larger angles of incidence. The angle-of-incidence effect was found to be greatest for the smaller deposit thicknesses and can be seen more clearly in Figs. 6a through d which are for wavelengths of 0.4, 0.6, 0.8, and 1.0 μ, respectively. In these figures, the reflectance is shown as a function of angle of incidence with deposit thickness as a parameter. For the bare surface (0.0-mm deposit thickness), the reflectance is fairly constant for incidence angles out to 40 deg. Beyond 40 deg the reflectance begins to increase rapidly and at 60 deg has essentially doubled. For small H_2O cryodeposit thicknesses, such as 0.11 and 0.22 mm in Figs. 6a through d, the reflectance is also seen to increase substantially with increasing angle of incidence. As the deposit thickens, the reflectance curves flatten out and become independent of the angle of incidence. At the greater deposit thicknesses, 0.88 and 1.32 mm, the reflectance is between 90 and 100 percent relative to the reflectance of MgO and is essentially independent of both angle of incidence and wavelength. At these thicknesses the reflectance has increased by a factor of 15 to 20 times that of the reflectance of the bare black epoxy paint surface.

The reflectance of the water cryodeposits varied somewhat with the test gas flow rate. For the lower flow rates, the reflectance curves were similar to those shown in Figs. 5 and 6. At a higher flow rate the data showed considerable absorption in the wavelength range from 0.8 to 1.1 μ. This is in the spectral region where the absorption coefficient of water is known to be appreciable (Ref. 6). Figure 7 shows the reflectance of water cryodeposits formed at the higher flow rate (1.44 x 10^{-3} gm/sec) on black epoxy paint and polished copper substrates. At wavelengths of 0.8 and, especially, 1.0 μ, there is a pronounced decrease in the reflectance from that observed in Fig. 5. The increased absorption is thought to be due to the higher flow rate, causing a change in the deposit formation properties, such as crystal structure or particle size. A similar absorption increase in this wavelength region was predicted by Dunkle and Bevans in their theoretical reflectance model for snow (Ref. 6). For a fixed absorption coefficient the reflectance in this spectral region was found to decrease greatly for increasing particle size.

For the three wavelengths considered in Fig. 7 (0.4, 0.8, and 1.0μ), there is a crossover of the reflectance curves for the copper and the black paint. Initially, the bare copper surface had a much higher reflectance than the black paint for all wavelengths. As the cryodeposit thickness increased, the reflectance curves at a given wavelength

crossed over and, for any further increase in thickness, the cryodeposit formed on the black paint exhibited a higher reflectance than a deposit of the same thickness formed on polished copper. Since the reflectance of the bare copper substrate was higher than that of black epoxy for all wavelengths, the only plausible explanation is that the deposit formed differently on the two surfaces. If the deposit had formed identically on the two surfaces, then it does not appear feasible that the black epoxy substrate and cryodeposit could attain a higher reflectance than the copper surface coated with a deposit of the same thickness. From Dorsey's discussion on the formation of ice and frost (Ref. 7), a possible explanation is that the deposit which formed on the black epoxy was crystalline in form, whereas the deposit formed on the copper may have been amorphous. Since the amorphous structure appears transparent or glassy, the reflectance would be less than that of the white crystalline frost observed on the black paint substrate. There is probably a mixture of both crystalline and amorphous forms in both cases, but one type may be more predominant for a particular substrate. The formation of amorphous ice on a copper surface at liquid air temperatures has been observed previously (Ref. 7). Dorsey points out the considerable research done on the formation of ice under various conditions. The results indicate that the ice structure will depend on the pressure at which the deposit is formed and especially on the temperature of the surface on which the ice is deposited.

3.3 CO$_2$ CRYODEPOSITS

The spectral reflectance of carbon dioxide cryodeposits in the visible and near infrared spectrum has been previously reported in Refs. 1, 3, and 4. In general, the reflectance of the CO$_2$ deposits was somewhat similar to that of water cryodeposits, although no absorption bands were found for CO$_2$ in the wavelength range from 0.36 to 1.15 μ. Over most of the wavelength range studied, the reflectance of the CO$_2$ cryodeposits was less than the water cryodeposit reflectance. In Fig. 8 the reflectances of CO$_2$ cryodeposits formed on a black epoxy substrate are shown as a function of deposit thickness and wavelength for angles of incidence of 0, 20, 40, and 60 deg. Again, as was the case for the water deposits, the reflectance was greatest for the shortest wavelength radiation and decreased with increasing wavelength. In Figs. 8a through d the $\lambda = 0.4 \mu$ curves are seen to be much higher than the 0.6 μ, which, in turn, is higher than the 0.8 μ curve. Again, a reflectance plateau was obtained for a deposit thickness of about 1 mm. A further increase in the thickness changed the reflectance only slightly. In Figs. 8a through d no intermediate points were taken for thicknesses

between 0.67 and 1.83 mm. However, other results not presented in this report have shown the reflectance versus thickness curves to be relatively smooth for CO_2 deposits. As was the case for water deposits, the curves in Fig. 8 for the four angles of incidence are similar in shape but different in magnitude. The effect of angle of incidence on CO_2 cryodeposit reflectance is further illustrated in Fig. 9, where the reflectance is plotted as a function of angle of incidence for deposit thicknesses of 0, 0.15, 0.30, 0.61, and 1.83 mm and for wavelengths of 0.4, 0.6, 0.8, and 1.0 μ. In contrast to what was found for the water cryodeposits, the reflectance was a strong function of the angle of incidence at the larger deposit thicknesses. For example, in Fig. 9d the reflectance of a 1.83-mm-thick deposit for 1.0 μ radiation is 85 percent at an angle of incidence of 60 deg, as compared with a reflectance value of 61 percent at normal incidence. In all of the curves shown in Fig. 9, this same trend can be seen. Unlike the water deposits, no effect of test gas flow rate was noted on the reflectance of CO_2 cryodeposits.

3.4 DISCUSSION OF ERRORS

For any particular sample, the experimental reflectance data were reproducible within ±0.005 for a low value and ±0.02 for a high value of reflectance. The cryodeposit reflectances were measured relative to the reflectance of MgO with the reference measurement being made before the formation of the cryodeposits. In any measurements made thereafter, it was assumed that the operating parameters of the optical system were the same as for the MgO reference measurements, i.e., the efficiency of the light source, integrating sphere and detector remained constant throughout the experiment. Although some changes were noted, the cryodeposit reflectance measurements were accurate to within ±3 percent.

The deposit thicknesses were calculated using Eq. (2), and the uncertainty in them depends almost entirely on the uncertainties in the deposit density and the mass flow rate of the test gas. Test gas flow rate can be measured accurately, but the cryodeposit densities are, in some cases, difficult to determine. Densities of CO_2 cryodeposits were reported in Ref. 2, but water cryodeposit densities have not been firmly established. Although these uncertainties exist, thickness measurements obtained from interference reflectance patterns indicate that the calculated deposit thicknesses are accurate to within ±10 percent for the H_2O deposits and ±5 percent for the CO_2 deposits.

8

SECTION IV
REPRESENTATION OF THICKNESS DEPENDENCE OF H_2O
CRYODEPOSIT REFLECTANCE USING EQUATIONS OF HULBURT

Hulburt has obtained an analytical solution for the forward and backward radiant fluxes in a scattering and absorbing medium (Ref. 8). In this study, his equations will be used to theoretically represent the thickness dependence of water cryodeposit reflectance. For normal collimated irradiance, the reflectance obtained from Hulburt's solution reduces to

$$R = \frac{(1 - \eta_c)\, \sigma_c\, \sinh \gamma\ell + \frac{b\ell}{i_0}\, D(\gamma\, \cosh \gamma\ell\ -\ A\, \sinh \gamma\ell - \gamma T)}{\gamma\, \cosh \gamma\ell + [(1 - \eta_d)\, \sigma_d + \beta_d]\, \sinh \gamma\ell} \qquad (3)$$

where

$$\frac{b\ell}{i_0} = \frac{r\,[\gamma C - T(CA - B - \beta_d)\, \sinh \gamma\ell - T(C - 1)\, \gamma\, \cosh \gamma\ell]}{(g + \beta_d)\, \sinh \gamma\ell + \gamma\, \cosh \gamma\ell}$$

$$A = \beta_c + \sigma_c$$

$$B = \eta_c \sigma_c\ +\ (1 - \eta_d)\, \sigma_d$$

$$C = \frac{\sigma_c\, [\eta_c\, (\beta_d + \beta_c + \sigma_c) + (1 - \eta_d)\, \sigma_d]}{(\beta_c + \sigma_c)^2 - \gamma^2}$$

$$D = \frac{\sigma_c\, [(1 - \eta_c)(\beta_d - \beta_c - \sigma_c) + (1 - \eta_d)\, \sigma_d]}{(\beta_c + \sigma_c)^2 - \gamma^2}$$

$$T = \exp\ -\ (\beta_c\ +\ \sigma_c)\, \ell$$

$$\gamma = [\beta_d\, \{2(1\ -\ \eta_d)\, \sigma_d\ +\ \beta_d\}]^{\frac{1}{2}}$$

$$g = (1\ -\ r)\, (1\ -\ \eta_d)\, \sigma_d$$

and the subscripts c and d refer to collimated and diffuse radiation, respectively. The attenuation coefficients of the medium due to absorption are β_c and β_d, the attenuation coefficients due to scattering are σ_c and σ_d, and the respective fractions of collimated and diffuse radiation scattered in the forward direction are η_c and η_d. The thickness of the medium is ℓ, and the reflectance of the diffusely scattering substrate is r.

In calculating the reflectance values of water cryodeposits, it was assumed that

$$\beta_d\ =\ 2\beta_c \text{ and } \sigma_d\ =\ 2\sigma_c \qquad (4)$$

9

which Hulburt shows to be true for uniformly diffuse radiation. The absorption coefficients, β_c, of ice were obtained from Sauberer (Ref. 9). For the black substrate, the value of the reflectance, r, was taken as 0.04 for all wavelengths. It was assumed that $\eta_d = 0.5$, i.e., the fraction of the diffuse radiation scattered backward is the same as that scattered forward. Also, it was assumed $\eta_c = 0.9$, which means that for collimated radiation, the particles in the deposit scatter strongly forward (Ref. 10). The scattering coefficient, σ_c, is not known for the water cryodeposit and would be difficult to determine since it depends in a complex manner on the effective size of the particles (particle diameter to wavelength ratio) in the deposit, their shape and their refractive indices. Even if all these variables were known, there is no exact solution for the scattering coefficient in a multiple scattering problem such as this one. Hence, σ_c was varied to find the best representation of the experimental results with the objective being to determine the validity of using Hulburt's equations for calculating cryodeposit reflectances as a function of thickness.

Figure 10 shows the theoretical representation of the experimental thickness dependence of water cryodeposit reflectances for wavelengths of 0.4, 0.6, and 0.8 μ. The experimental reflectances presented in this figure are the relative experimental values converted to absolute values by assuming that the reflectance of the MgO was 0.96 at all wavelengths. From Fig. 10, it is seen that at the larger deposit thicknesses, $\ell > 0.22$ mm, Hulburt's equations give a good representation of the experimental results for all three wavelengths. The experimental point at 1.32 mm is an exception but, as mentioned earlier, the deposit of this particular thickness probably had a crystal structure which was quite different from that of the thinner deposits. Neglecting this experimental point, the largest difference between the theoretical and experimental results for thick deposits ($\ell > 0.44$ mm) is only 5.7 percent. Most of this difference is within experimental uncertainty. For thin deposits ($\ell < 0.2$ mm), agreement should not be expected between the theoretical and experimental results because Hulburt's formulation does not take into account the effects of interference (Refs. 1 and 2) and individual particle scattering (Ref. 11), i.e., phase differences between various rays in the deposit. However, the extent of the thickness region for which these effects are important is probably limited by the effective deposit thickness (thickness to wavelength ratio). If such is the case, the thickness at which theoretical and experimental results would begin to agree should decrease as the wavelength of the incident radiation decreases. This is indeed seen to occur in Fig. 10.

SECTION V
CONCLUSIONS

The following conclusions can be drawn from this study of the spectral optical reflectance properties of water and carbon dioxide cryodeposits:

1. Reflectances of from 75 to 100 percent relative to MgO were obtained for H_2O and CO_2 deposits 1 to 2 mm thick. These values indicate that the presence of cryodeposits on LN_2-cooled space chamber walls could substantially increase the radiation load on a test vehicle.

2. Water and CO_2 cryodeposit reflectances are strongly dependent on thickness up to approximately 1 mm. A further increase in thickness results in a relatively small reflectance change.

3. Carbon dioxide deposit reflectances depend strongly on the angle of incident radiation for all thicknesses, whereas H_2O reflectances are essentially independent of the incidence angle for large deposit thicknesses.

4. Thin film interference effects were observed for thin films of both H_2O and CO_2 formed on polished copper and black painted surfaces. In most cases the presence of the film caused a decrease in the reflectance.

5. Water cryodeposit reflectances showed a dependence on the test gas flow rate and/or pressure at which the deposits were formed. At the higher flow rate, an increase in absorption was observed in the wavelength range from 0.8 to 1.0 μ with little change, if any, for other wavelengths. The increased absorption was probably due to an increase in particle size. No significant dependence on flow rate was seen for the CO_2 deposits.

6. The model developed by Hulburt (Ref. 8) for absorbing and scattering media can be used to represent the reflectance dependence on thickness for H_2O cryodeposits thicker than 0.22 mm.

REFERENCES

1. Wood, B. E., Smith, A. M., and McCullough, B. A. "The Spectral Reflectance of Water and Carbon Dioxide Cryodeposits from 0.36 to 1.15 Microns." AEDC-TR-67-131 (AD657018), August 1967.

2. Tempelmeyer, K. E., Wood, B. E., and Mills, D. W., Jr. "In Situ Measurement of Thickness and Other Properties of Carbon Dioxide Cryodeposits by Optical Techniques." AEDC-TR-67-226 (AD662869), December 1967.

3. McCullough, B. A., Wood, B. E., Smith, A. M., and Birkebak, R. C. "A Vacuum Integrating Sphere for In Situ Reflectance Measurements at 77°K from 0.5 to 10 Microns." Progress in Astronautics and Aeronautics, Volume 20, Academic Press, New York and London, 1967.

4. Wood, B. E., McCullough, B. A., Dawson, J. P., and Birkebak, R. C. "Vacuum Integrating Spheres for Measuring Cryodeposit Reflectances from 0.35 to 15 Microns." AEDC-TR-65-178 (AD468608), August 1965.

5. Handbook of Chemistry and Physics. Chemical Rubber Publishing Company, Cleveland, Ohio, 1958, (39th Edition).

6. Dunkle, R. V. and Bevans, J. T. "An Approximate Analysis of the Solar Reflectance and Transmittance of a Snow Cover." Journal of Meteorology, Vol. 13, 1956, pp. 212-216.

7. Dorsey, N. E. Properties of Ordinary Water-Substance. Reinhold Publishing Corporation, New York, 1940.

8. Hulburt, E. O. "Propagation of Radiation in a Scattering and Absorbing Medium." Journal of the Optical Society of America, Vol. 33, No. 1, January 1943, pp. 42-45.

9. "University of Minnesota, 1951: Review of the Properties of Snow and Ice." SIPRE Report 4, Institute of Technology, EES, Minneapolis, Minnesota, p. 156.

10. Plass, G. N. and Kattawar, G. W. "Monte Carlo Calculations of Light Scattering from Clouds." Applied Optics, Vol. 7, No. 3, March 1968, pp. 415-419.

11. Van de Hulst, H. C. Light Scattering by Small Particles. John Wiley and Sons, Inc., New York, 1964.

APPENDIX
ILLUSTRATIONS

MgO

Cryosurface

Photomulti-
plier Tube

LN$_2$ Transfer
Lines

Thermocouple Gage

Ionization Gage

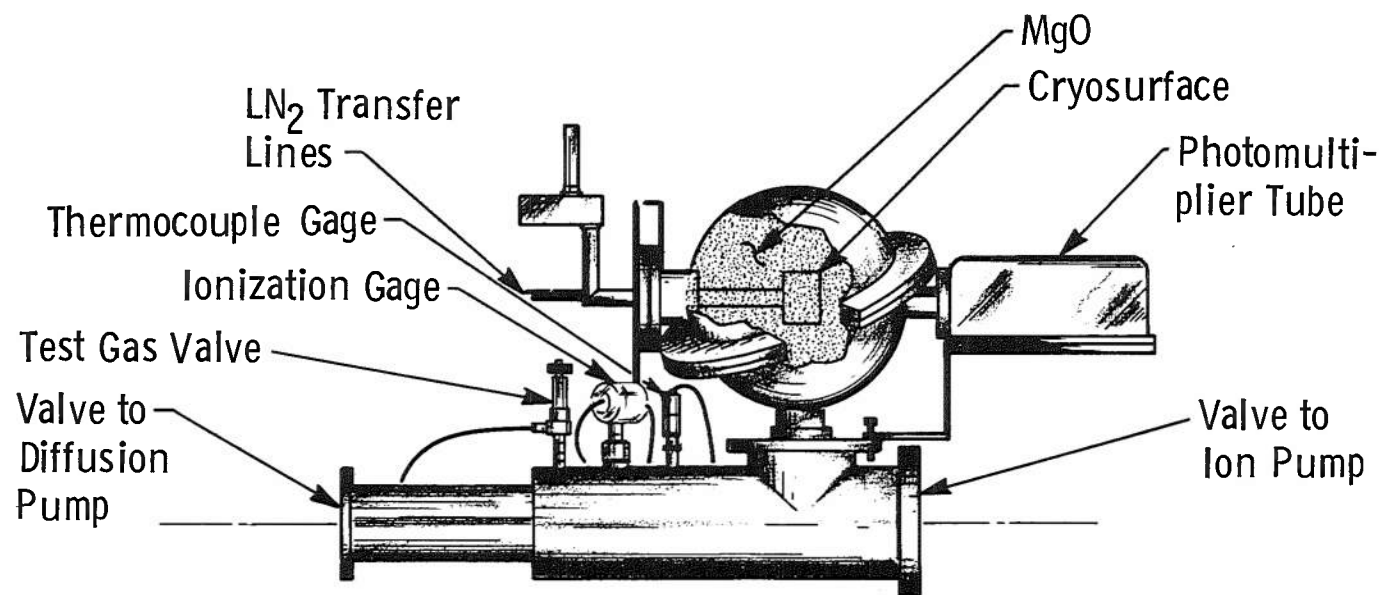Test Gas Valve

Valve to
Diffusion
Pump

Valve to
Ion Pump

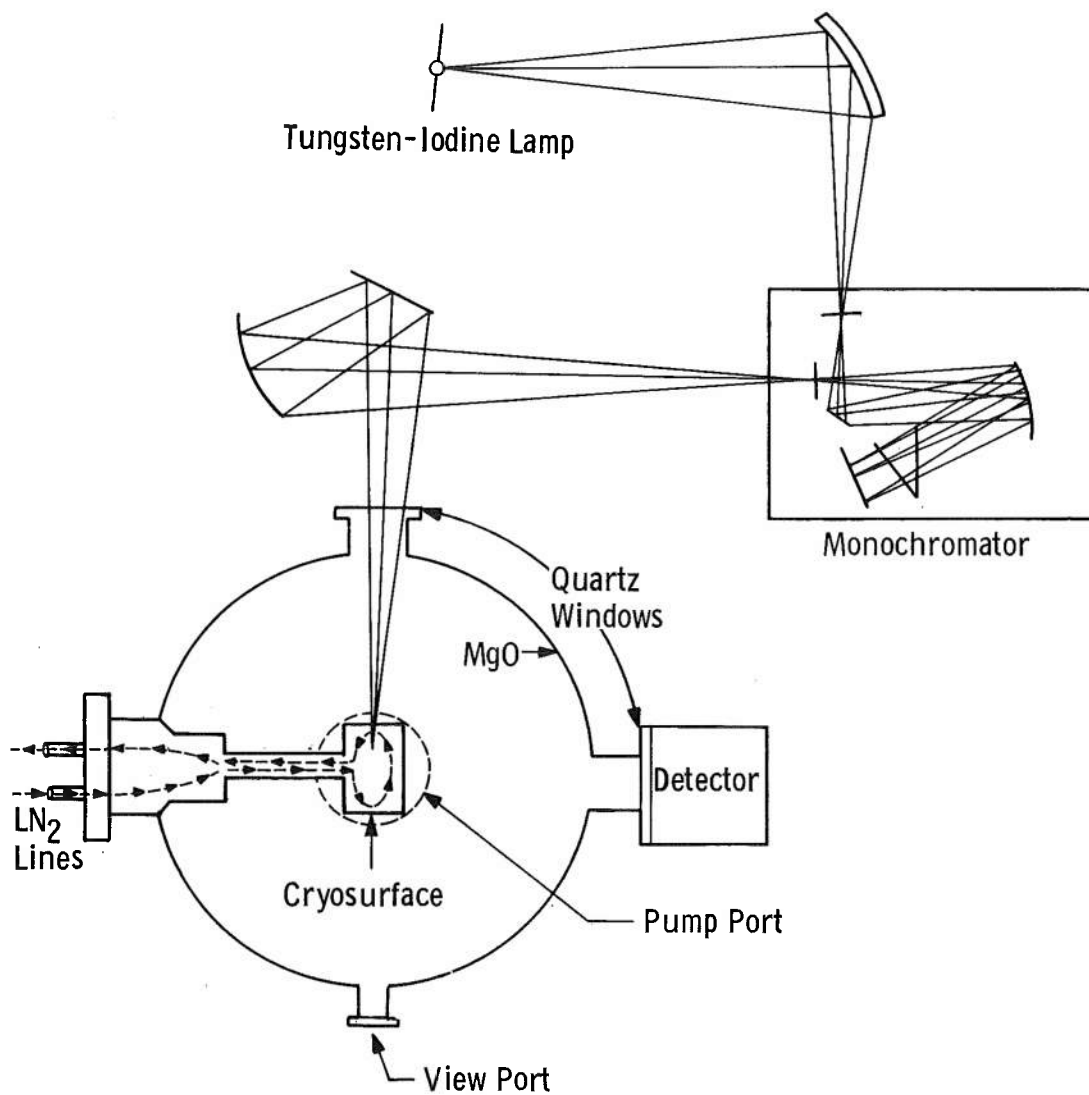Fig. 1 Drawing of 12-in. Integrating Sphere

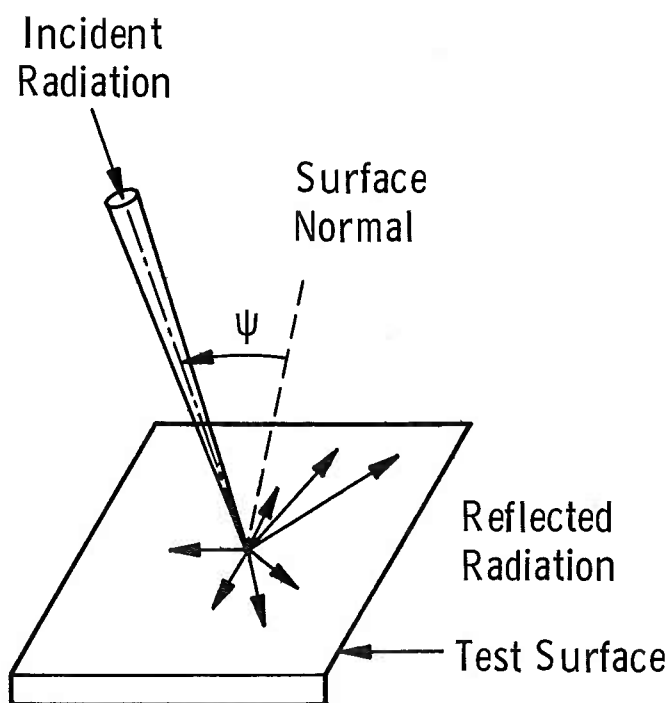**Fig. 2 12-in. Integrating Sphere and Optical System**

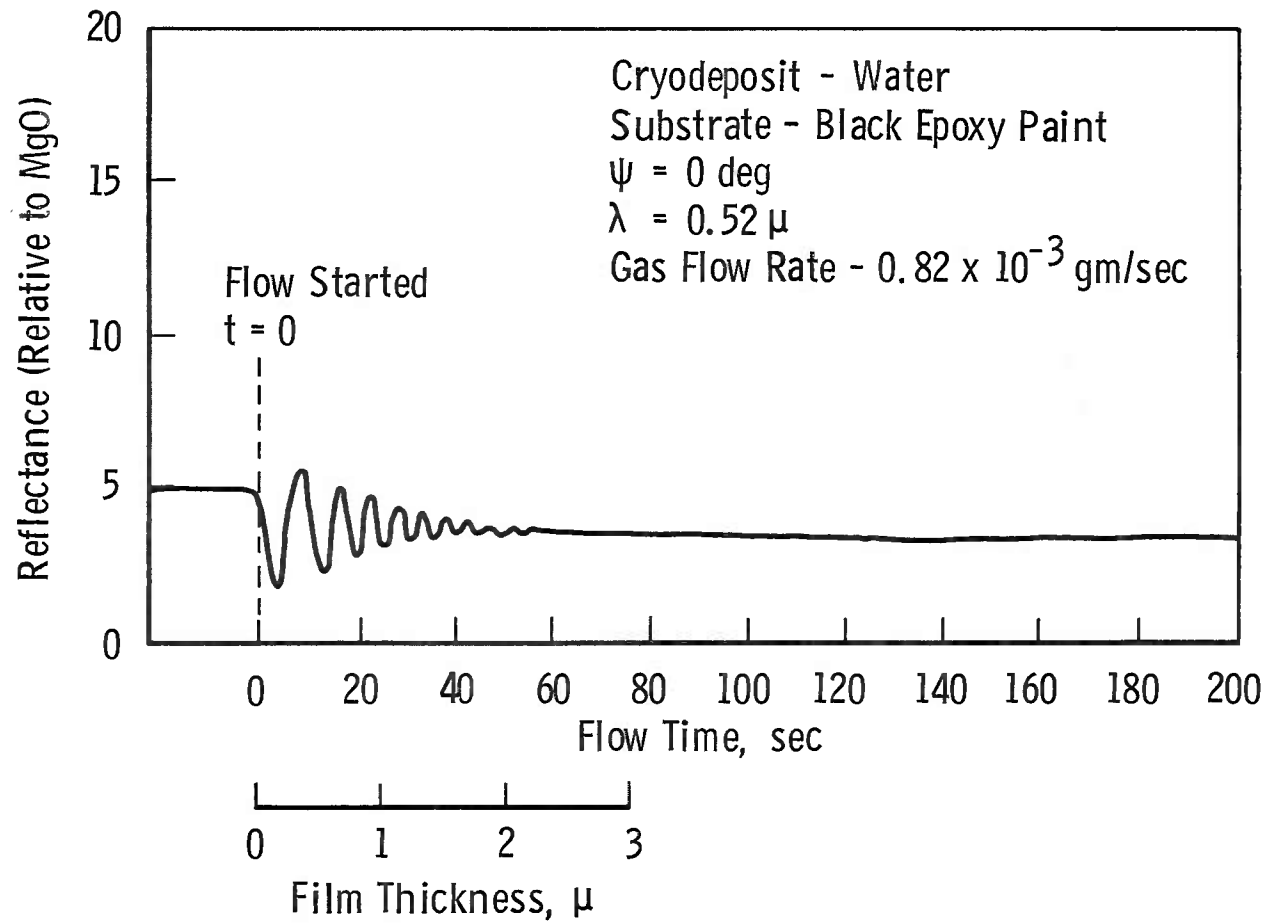Fig. 3 Angular-Hemispherical Reflectance Measurement Technique

Fig. 4 Interference Patterns Observed for Thin Water Cryodeposit Film

Cryodeposit – Water
Substrate – Black Epoxy Paint
Flow Rate – 1.01 x 10^{-3} gm/sec
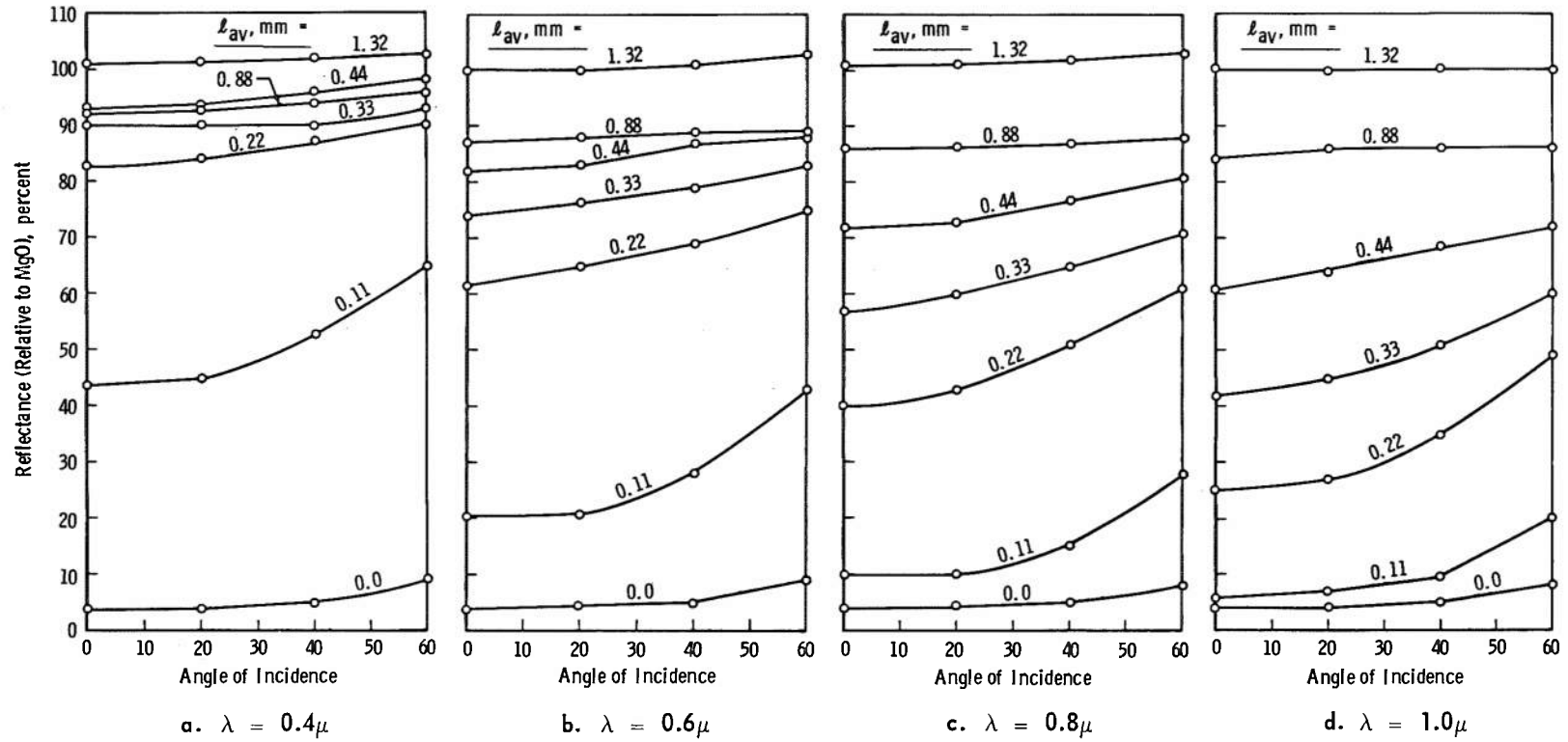

a. $\Psi = 0$ deg

b. $\Psi = 20$ deg

c. $\Psi = 40$ deg

d. $\Psi = 60$ deg
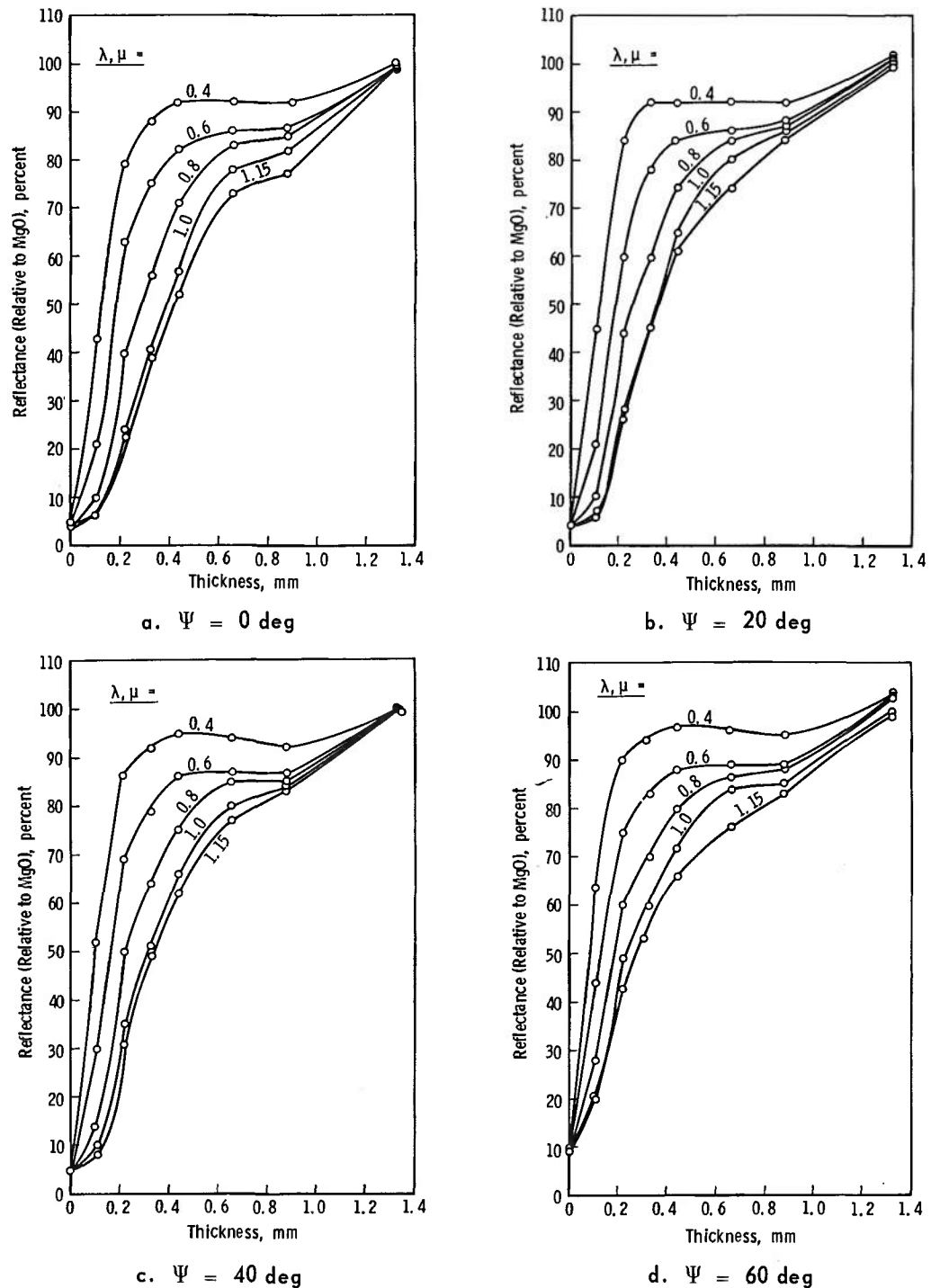
Fig. 5 Dependence of Water Cryodeposit Reflectance on Deposit Thickness

19

Cryodeposit - Water
Substrate - Black Epoxy Paint
Flow Rate - 1.01 x 10⁻³ gm/sec

a. $\lambda = 0.4\mu$

b. $\lambda = 0.6\mu$

c. $\lambda = 0.8\mu$

d. $\lambda = 1.0\mu$

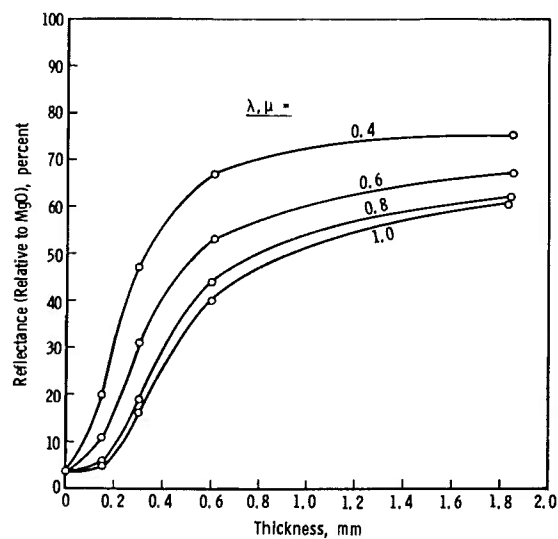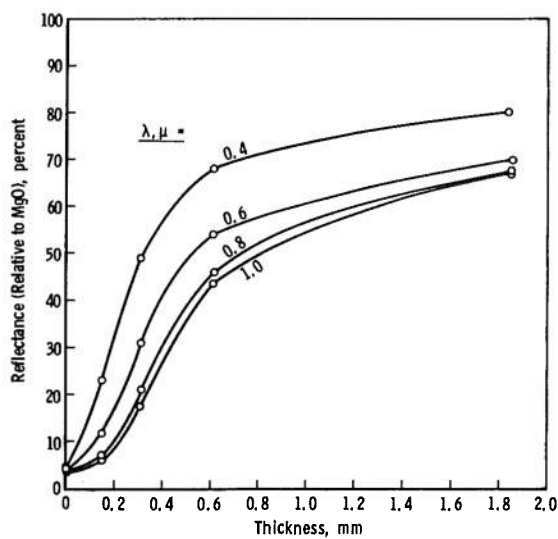Fig. 6 Dependence of Water Cryodeposit Reflectance on Incidence Angle, ψ
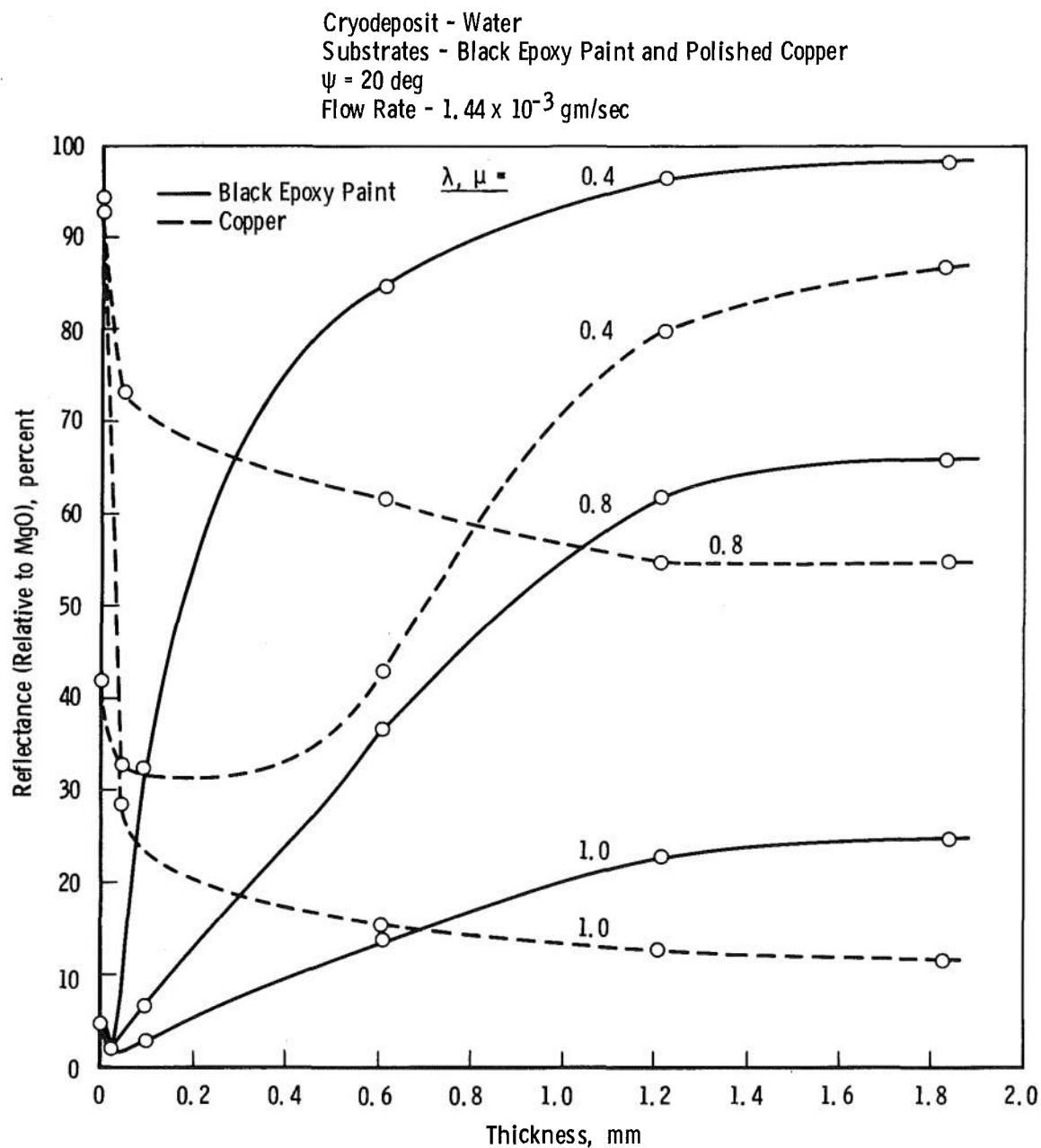
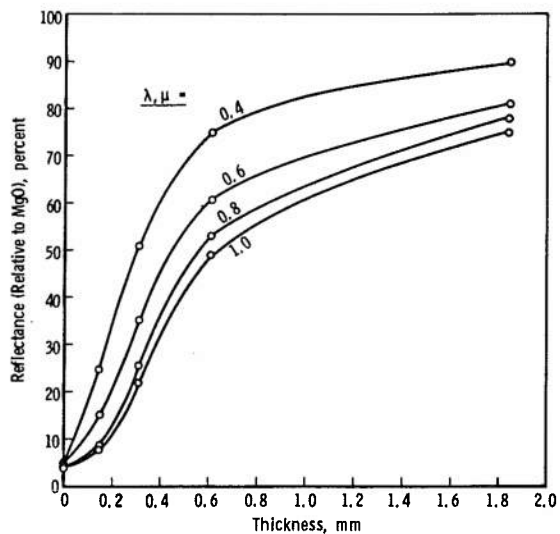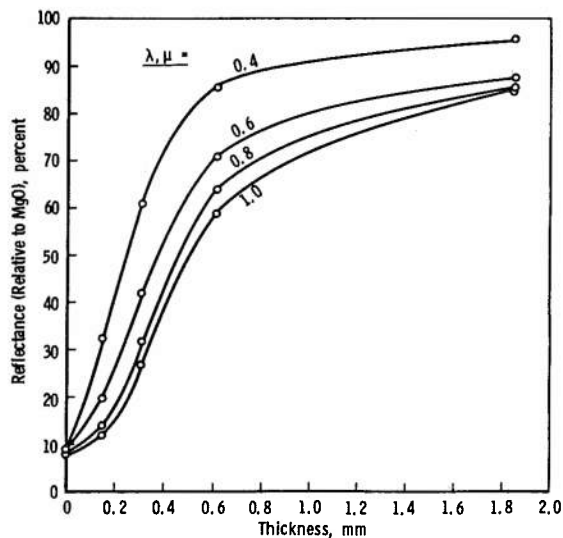Fig. 7 Reflectance of Water Cryodeposits Formed on Copper and Black Epoxy
Paint Substrates at a Flow Rate of 1.44 x 10⁻³ gm/sec

Fig. 8 Dependence of CO_2 Cryodeposit Reflectance on Deposit Thickness

Cryodeposit – Carbon Dioxide
Substrate – Black Epoxy Paint
Flow Rate – 2.4×10^{-3} gm/sec

a. $\lambda = 0.4\mu$

b. $\lambda = 0.6\mu$
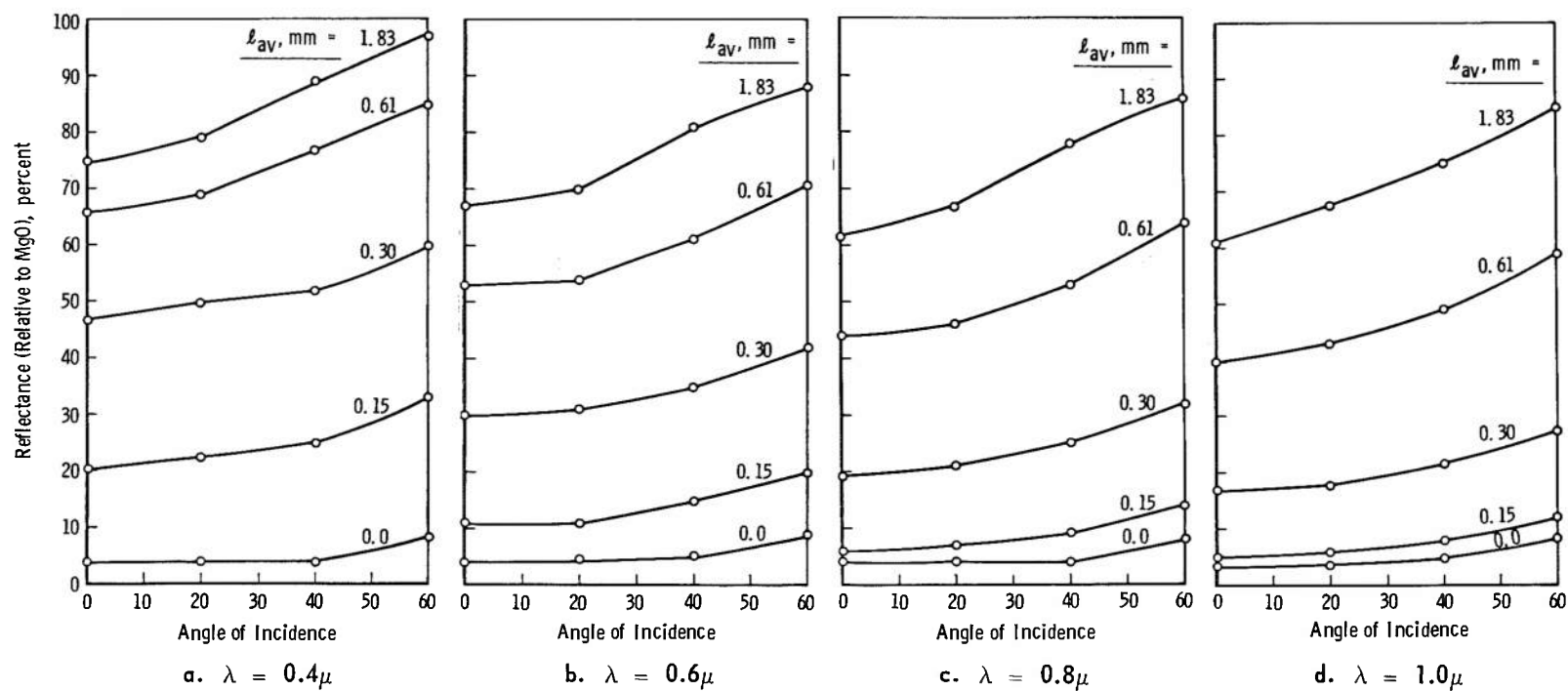
c. $\lambda = 0.8\mu$

d. $\lambda = 1.0\mu$

Fig. 9 Dependence of CO_2 Cryodeposit Reflectance on Incidence Angle, ψ
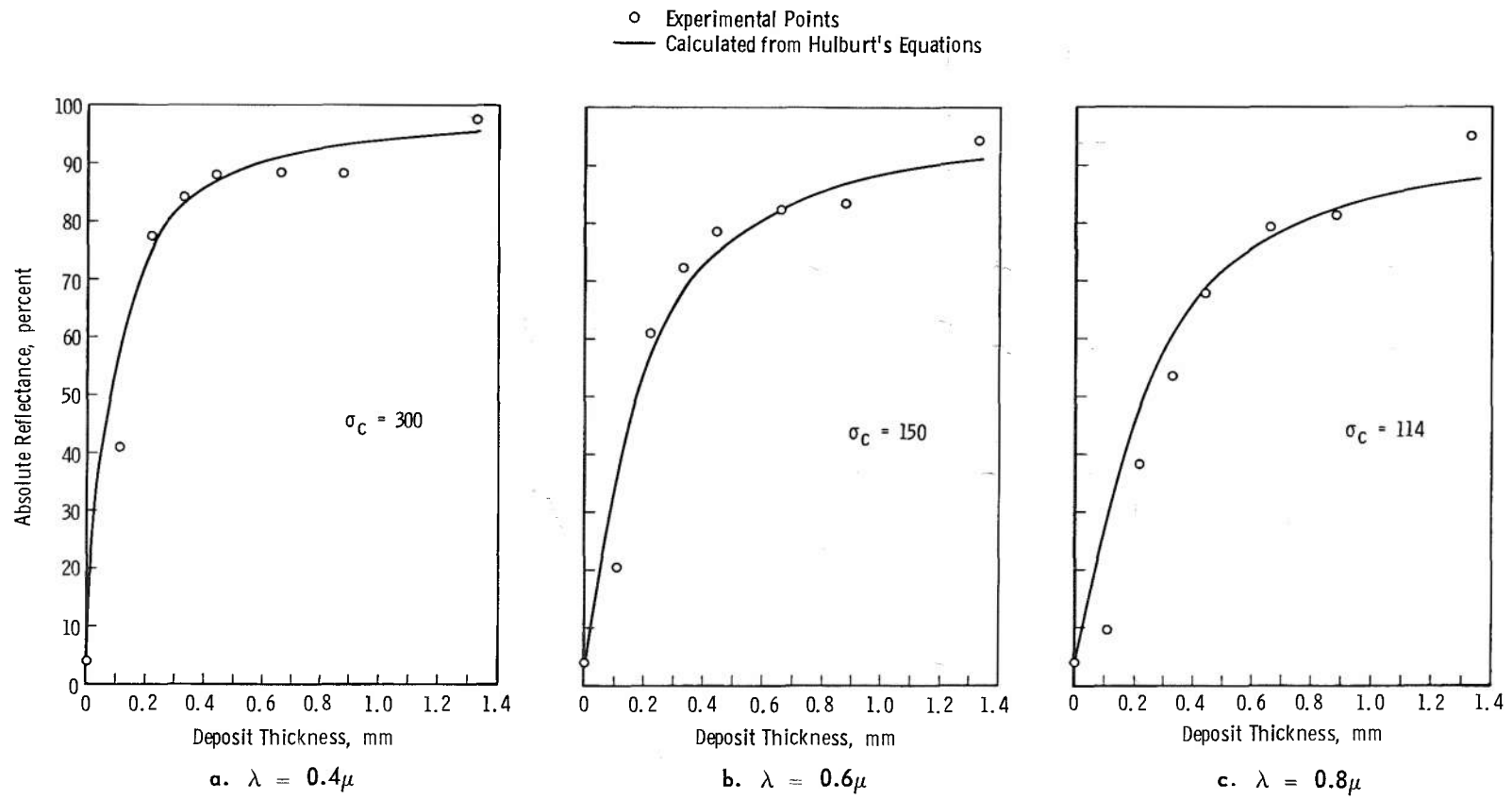
Fig. 10 Representation of the Experimental Thickness Dependence of Water
Cryodeposit Reflectance by the Equations of Hulburt

DOCUMENT CONTROL DATA - R & D

(Security classification of title, body of abstract and indexing annotation must be entered when the overall report is classified)

1. ORIGINATING ACTIVITY (Corporate author)	2a. REPORT SECURITY CLASSIFICATION
Arnold Engineering Development Center ARO, Inc., Operating Contractor Arnold Air Force Station, Tennessee	UNCLASSIFIED
	2b. GROUP N/A

3. REPORT TITLE

VARIATION OF H_2O AND CO_2 CRYODEPOSIT REFLECTANCES WITH ANGLE OF INCIDENCE AND DEPOSIT THICKNESS

4. DESCRIPTIVE NOTES *(Type of report and inclusive dates)*
May 1966 to April 1968 - Final Report

5. AUTHOR(S) *(First name, middle initial, last name)*

B. E. Wood, A. M. Smith, and B. A. Seiber, ARO, Inc.

6. REPORT DATE	7a. TOTAL NO. OF PAGES	7b. NO. OF REFS
September 1968	30	12

8a. CONTRACT OR GRANT NO. F40600-69-C-0001	9a. ORIGINATOR'S REPORT NUMBER(S)
b. PROJECT NO. 8951	AEDC-TR-68-144
c. Program Element 6144501F	9b. OTHER REPORT NO(S) (Any other numbers that may be assigned this report) N/A
d. Task 895104	

10. DISTRIBUTION STATEMENT

This document has been approved for public release and sale; its distribution is unlimited.

11. SUPPLEMENTARY NOTES	12. SPONSORING MILITARY ACTIVITY
Available in DDC	Arnold Engineering Development Center, Air Force Systems Command, Arnold Air Force Station, Tennessee

13. ABSTRACT

Cryodeposits which form on the cryogenically cooled walls of a space simulation chamber can change the wall reflectance and thus alter the thermal balance of the test vehicle. In this study, H_2O and CO_2 cryodeposits of thicknesses up to 1.8 mm were formed on a $77^\circ K$ surface under vacuum. The spectral reflectances of these deposits were measured in situ with an integrating sphere for angles of incidence from 0 to 60 deg. At the smaller deposit thicknesses, the reflectance showed a strong dependence on both thickness and angle of incidence, whereas at larger thicknesses the dependence was less. A theoretical model developed for reflectance determination of absorbing and scattering media gives a good representation of the thickness dependence of water cryodeposit reflectance except at very small thicknesses where interference effects are known to occur.

DD $\underset{1 \text{ NOV } 65}{\text{FORM}}$ 1473

14. KEY WORDS	LINK A		LINK B		LINK C	
	ROLE	WT	ROLE	WT	ROLE	WT
H_2O and CO_2 cryodeposits						
space simulation chamber						
vacuum						
spectral reflectances						
angle of incidence						
deposit thickness						
frosts						
low temperature						

1. water - carbondioxide.

2. Cryodeposits - Reflectance.

3.   "   - Effects.

/5 - 2.